Supporting Information

Photoreactivity of Metal-organic Frameworks in Aqueous Solutions: Metal Dependence of Reactive Oxygen Species Production

Kai Liu,[†] Yanxin Gao,[†] Jing Liu,[‡] Yifan Wen,[†] Yingcan Zhao,[§] Kunyang Zhang,[†] and Gang Yu[†,*]

[†] School of Environment, Beijing Key Laboratory for Emerging Organic Contaminants Control, State Key Joint Laboratory of Environmental Simulation and Pollution Control, Tsinghua University, Beijing 100084, China

[‡] MOE Key Lab of Environmental Remediation and Ecosystem Health, College of Environmental and Resource Sciences, Zhejiang University, Hangzhou 310058, China

[§] Lyles School of Civil Engineering and Division of Environmental and Ecological Engineering, Purdue University, West Lafayette, Indiana 47907, United States

Summary:

Pages: 9

Tables: 2

Figures: 15

Equations: 2

Table S1. Components of simulated river water used.

Anions	**Concentration (mg/L)**
Chloride	38.5
Phosphate	1.1
Nitrate	39.4
Sulfate	53.2

Table S2. Compounds detected after 5 h release of MIL-53(Fe) encapsulated diclofenac.

Compounds	**CAS**	**Structure**	**Retention time (min)**	**measured *m/z***	**M-H**	**Error (ppm)**	**Fragments (*m/z*)**	**Fragment Structures**	**Predicted formula (fragments)**
2-(8-Hydroxy-9H-carbazol-1-yl)acetic acid	131023-45-5	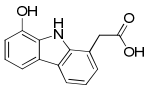	6.516	240.0667	$C_{14}H_{10}NO_3$	0.3	196.0771		$C_{13}H_{11}NO$ (1.6)
2-(9H-carbazol-1-yl)acetic acid	131023-43-3	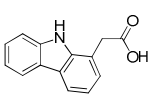	7.620	224.0716	$C_{14}H_{11}NO_2$	-0.5	180.0824		$C_{13}H_{11}N$ (2.9)
2-(8-chloro-9H-carbazol-1-yl)acetic acid	131023-44-4	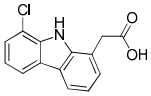	8.811	258.0325	$C_{14}H_{10}NO_2Cl$	-0.9	214.0431		$C_{13}H_{10}NCl$ (0.9)
Diclofenac	15307-79-6	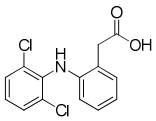	9.767	294.0091	$C_{14}H_{10}NO_2Cl_2$	-1.0	250.0195	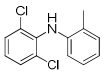	$C_{13}H_{11}NCl_2$ (-0.3)

Figure S1. PXRD patterns of as-synthesized isoreticular MIL-53s.

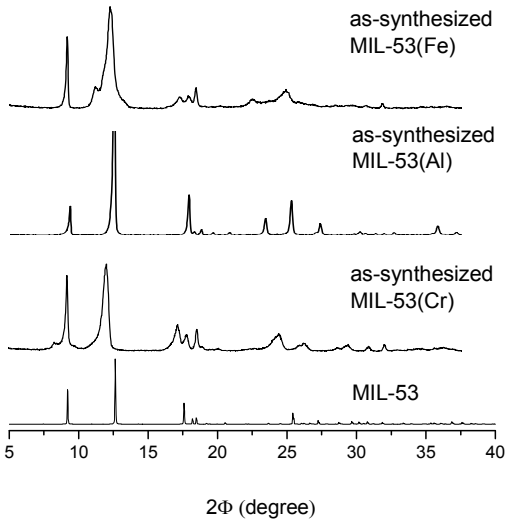

Figure S2. SEM of as-synthesized MIL-53(Cr) (left), MIL-53(Al) (middle), and MIL-53(Fe) (right).

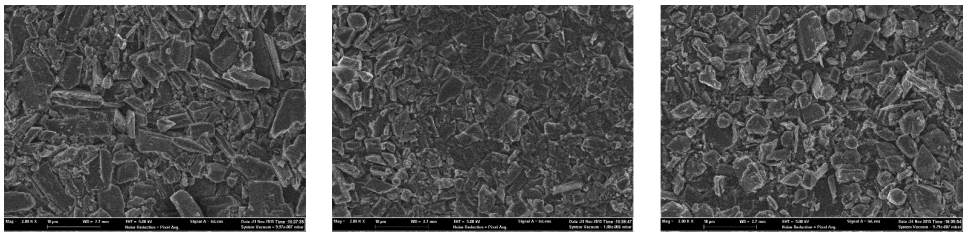

Figure S3. PXRD of different MIL-53s immersed in buffered mili-Q water at pH 7.0 and exposed to sunlight irradiation.

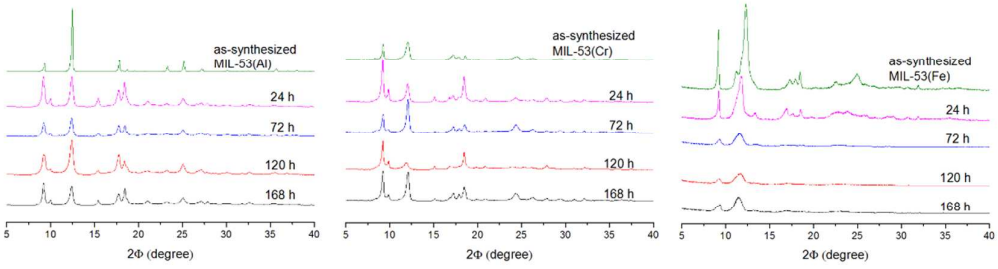

Figure S4. PXRD of different MIL-53s immersed in buffered mili-Q water at pH 7.0 and exposed to lamp irradiation.

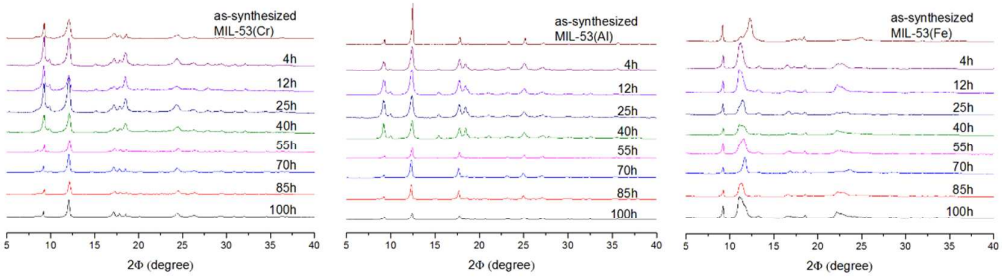

Figure S5. Evidence of $^1O_2$ production by FFA (0.2 mM) reduction at pH 7.0 under sunlight irradiation at the presence of MIL-53(Cr) (□), MIL-53(Al) (○), MIL-53(Fe) (◊), and FFA alone (+)

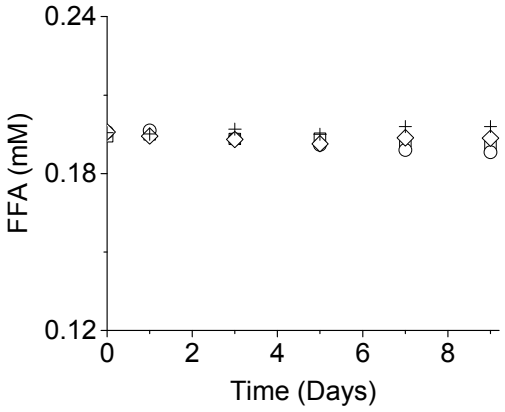

Figure S6. $O_2^{\cdot-}$ formation detected by NBT^{2+} (0.2 mM) reduction at pH 7.0 under sunlight irradiation at the presence of MIL-53(Cr) (□), MIL-53(Al) (○), MIL-53(Fe) (◊), and NBT^{2+} alone (+).

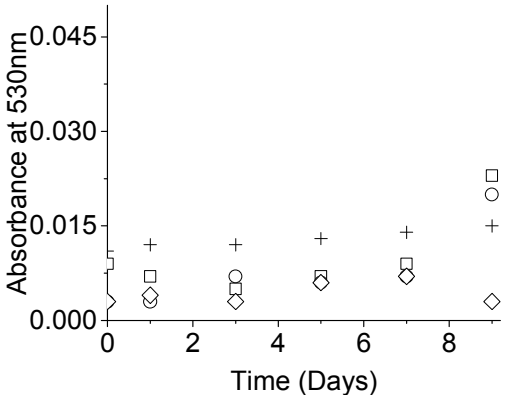

Figure S7. ·OH formation detected by *p*CBA (5 μM) reduction at pH 7.0 under sunlight irradiation at the presence of 10 mg/L solution of MIL-53(Cr) (□), MIL-53(Al) (○), MIL-53(Fe) (◊), and *p*CBA alone (+).

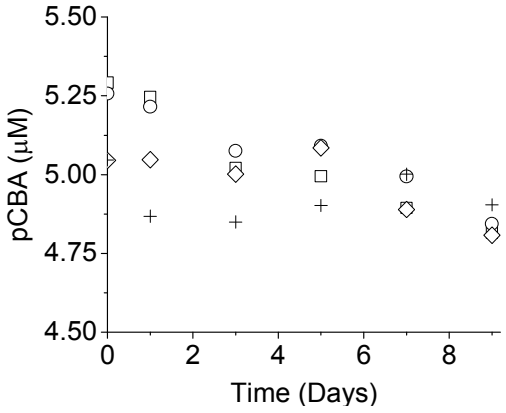

Figure S8. Adsorption kinetics of diclofenac on MIL-53(Fe) at pH 7.0.

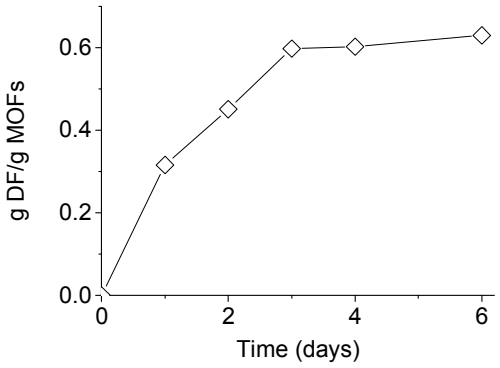

Figure S9. HPLC analysis of blank sample (diclofenac solution without MOFs) irradiated under lamp at predetermined time.

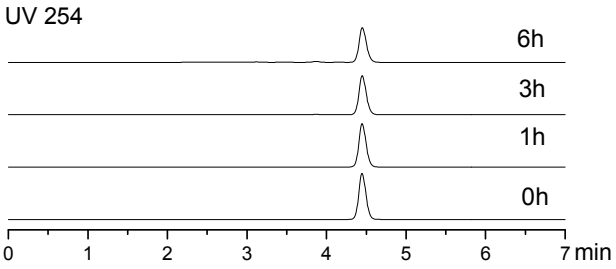

Figure S10. Diclofenac delivery and subsequent transformation by MIL-53(Fe) at the presence of lamp irradiation at pH 7.0.

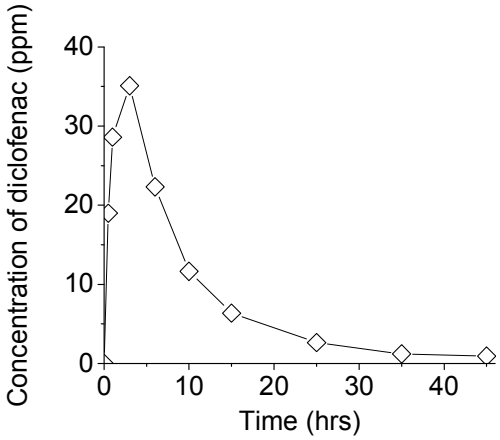

Figure S11. Proposed MIL-53(Fe) encapsulated diclofenac transformation pathway.

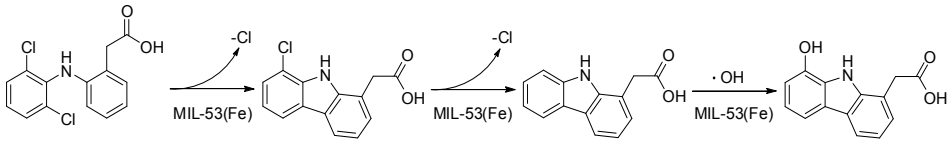

Figure S12. Mass spectrum of transformation product 2-(8-Hydroxy-9H-carbazol-1-yl)acetic acid released from MIL-53(Fe) encapsulated diclofenac, analyzed by Q-TOF LC/MS (ESI-)

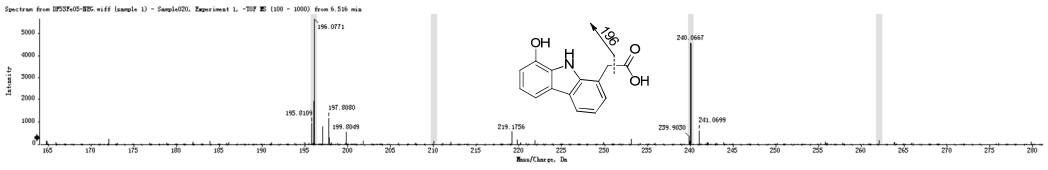

Figure S13. Mass spectrum of transformation product 2-(9H-carbazol-1-yl)acetic acid released from MIL-53(Fe) encapsulated diclofenac, analyzed by Q-TOF LC/MS (ESI-)

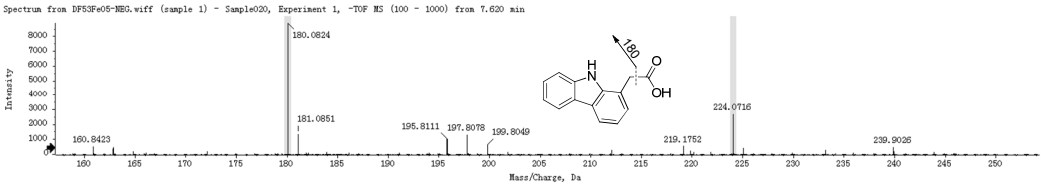

Figure S14. Mass spectrum of transformation product 2-(8-chloro-9H-carbazol-1-yl)acetic acid released from MIL-53(Fe) encapsulated diclofenac, analyzed by Q-TOF LC/MS (ESI-)

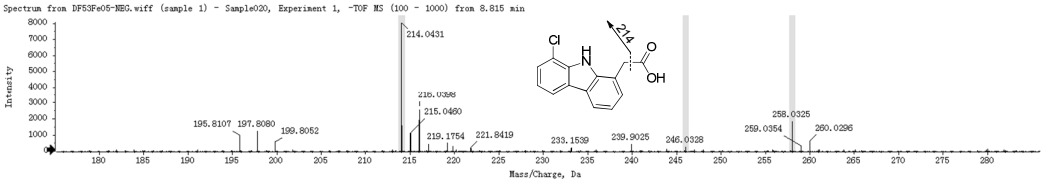

Figure S15. Mass spectrum of diclofenac released from MIL-53(Fe) encapsulated diclofenac, analyzed by Q-TOF LC/MS (ESI-)

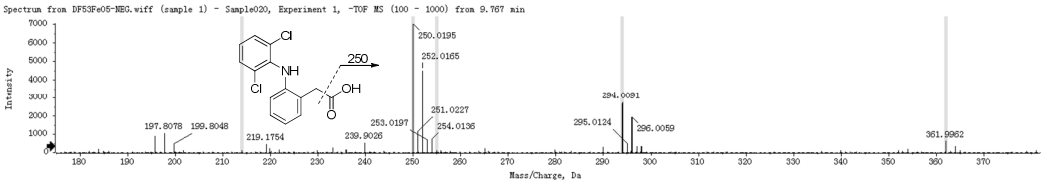

ROS Measurements

$^1O_2$ Measurement

In accordance to previous literature,[1] the steady-state concentration of $^1O_2$ is measured by eq S1:

$$-\frac{d[FFA]}{dt} = k_r\left[\,{}^1O_2\right]_{ss}[FFA]$$

$$-\frac{d[FFA]}{dt} = k_{ex}[FFA]$$

$$\left[\,{}^1O_2\right]_{ss} = \frac{k_{ex}}{k_r} \qquad \text{(S1)}$$

where k_{ex} is the pseudo-first-order rate constant derived from the experiment, and k_r is 1.2×10^8 M^{-1} s^{-1}.

·OH Measurement

Due to the low concentration of pCBA used (5 μM), the reaction between pCBA and hydroxyl radical ·OH appears pseudo-first-order (Figure 3). In accordance to the previous literature,[1] the steady-state concentration of ·OH is measured by rate law that is analogous to eq S1:

$$-\frac{d[pCBA\,]}{dt} = k_r[\cdot OH]_{ss}[pCBA]$$

$$-\frac{d[pCBA]}{dt} = k_{ex}[pCBA]$$

$$[\cdot OH\,]_{ss} = \frac{k_{ex}}{k_{pCBA}} \qquad \text{(S2)}$$

where k_{ex} is the pseudo-first-order rate constant derived from the experiment, and k_r is 5.2×10^9 M^{-1} s^{-1}.

Literature Cited

(1) Chen, C.-Y.; Jafvert, C. T., Photoreactivity of Carboxylated Single-Walled Carbon Nanotubes in Sunlight: Reactive Oxygen Species Production in Water. *Environmental Science & Technology* **2010,** *44*, (17), 6674-6679.